Electronic Supplementary Material (ESI) for CrystEngComm.
This journal is © The Royal Society of Chemistry 2021

Driving a sustainable application of s-triazines Ametryn and Atrazine herbicides through multicomponent crystals with improved solubility

*Amandha Kaiser da Silva[a], Luan F. Diniz[b], Juan C. Tenorio[c], Carlos E. D. Nazario[a], Caue Ribeiro[d], Paulo de Sousa Carvalho Jr[e]**

[a]Instituto de Química, Universidade Federal do Mato Grosso do Sul, 79074-460, Campo Grande, MS, Brazil.[b]Laboratório de Controle de Qualidade, Departamento de Produtos Farmacêuticos, Faculdade de Farmácia, Universidade Federal de Minas Gerais, 31270-901, Belo Horizonte, MG, Brazil. [c]Instituto de Química, Universidade Estadual de Campinas, 13083-970, Campinas, SP, Brazil. [d]National Nanotechnology Laboratory for Agribusiness (LNNA), EMBRAPA Instrumentação, 13560-970, São Carlos, SP, Brazil. [e]Instituto de Física, Universidade Federal do Mato Grosso do Sul, 79070-900, Campo Grande, MS, Brazil. *e-mail: paulo.sousa@ufms.br

Table S1. Crystal data and structure refinement parameters for the s-triazine organic salts.

	ATZ-H_2Fum·H_2O	**ATZ-H_2Fum**	**AMT-NO3**	**AMT-TFA**
Empirical formula	$C_{10}H_{16.22}ClN_5O_{2.11}$	$C_{10}H_{16}ClN_5O_2$	$C_9H_{18}N_6O_3S$	$C_{11}H_{18}F_3N_5O_2S$
Formula weight	275.71	273.73	290.35	341.36
Temperature (K)	120.0	120.0	298.0	298.0
Crystal system	Monoclinic	Monoclinic	Triclinic	Monoclinic
Space group	*C*2/c	*C*2/c	$P\bar{1}$	$P2_1/c$
a/Å	18.892(4)	18.922(13)	9.1659(7)	8.2238(3)
b/Å	6.2547(15)	6.297(4)	9.5067(8)	10.1689(3)
c/Å	24.173(6)	24.311(16)	9.6825(8)	19.8066(5)
α/°	90	90	77.541(7)	90
β/°	104.589(4)	104.748(6)	72.346(7)	99.017(3)
γ/°	90	90	67.479(7)	90
Volume/Å^3	2764.3(11)	2801(3)	737.90(11)	1635.90(9)
Z	8	8	2	4
ρcalcg/cm3	1.325	1.298	1.307	1.386
μ/mm^{-1}	0.281	0.276	0.234	0.241
F(000)	1161.0	1152.0	308.0	712.0
Crystal size/mm^3	0.222 × 0.14 × 0.08	0.239 × 0.149 × 0.052	0.52× 0.38 × 0.3	0.34 × 0.22 × 0.03
2Θ range for data collection/°	6.31 to 53.46	6.3 to 52.724	6.802 to 53.438	6.988 to 54.968
Index ranges	$-23 \leq h \leq 23$, $-7 \leq k \leq 7$, $-30 \leq l \leq 30$	$-22 \leq h \leq 23$, $-7 \leq k \leq 7$, $-30 \leq l \leq 30$	$-11 \leq h \leq 11$, $-12 \leq k \leq 11$, $-12 \leq l \leq 12$	$-10 \leq h \leq 10$, $-11 \leq k \leq 13$, $-25 \leq l \leq 25$
Reflections collected	28552	38166	15139	20777
Independent reflections	2928 [R_{int}= 0.2164, R_{sigma}= 0.0811]	2851 [R_{int}= 0.0743, R_{sigma}= 0.0306]	3125 [R_{int}= 0.0288, R_{sigma}= 0.0198]	3703 [R_{int}= 0.0320, R_{sigma}= 0.0236]
Data/restraints/parameters	2928/36/179	2851/36/167	3125/58/204	3703/0/203
Goodness-of-fit on F^2	1.079	1.093	1.046	1.041
Final R indexes [I>=2σ (I)]	R1= 0.0865, wR2= 0.22249	R1= 0.0889, wR2= 0.2619	R1= 0.0657, wR2= 0.1806	R1= 0.0711, wR2= 0.2156
Final R indexes [all data]	R1= 0.0972, wR2= 0.2348	R1= 0.0984, wR2= 0.2714	R1= 0.0861, wR2= 0.1951	R1= 0.0948, wR2= 0.2365
Largest diff. peak/hole / e Å^{-3}	0.65/-0.89	0.84/-1.27	0.34/-0.24	0.92/-0.45

Table S2. H-bond and intermolecular interactions for the s-triazine organic salts.

D–H•••A	H•••A	D•••A	D–H•••A	Symmetry code
		ATZ-H_2Fum·H_2O		
O1–H1•••N1	2.674(4)	1.859(3)	172.17(2)	*x,y,z*
N2–H2•••O2	2.931(5)	2.079(3)	170.61(2)	*x,y,z*
C7–H7C•••OW1	3.222(3)	2.273(3)	169.40(8)	*x,y,z*
OW1–HW1B•••N3	3.388(3)	2.709(3)	137.99(2)	*x,y,z*
N5–H5•••N4	3.040(4)	2.181(3)	176.78(2)	*-x+2,+y,-z+1/2+1*
C10–H10•••OW1	3.622(3)	2.865(3)	139.37(7)	*-x+1/2+1,+y-1/2,-z+1/2+1*
C5–H5C•••O2	3.624(6)	2.705(3)	160.45(3)	*x+1/2,+y-1/2,+z*
		ATZ-H_2Fum		
N2–H2•••O2	2.943(6)	2.091(4)	170.69(3)	*x,y,z*
O1–H1•••N1	2.686(5)	1.871(4)	172.58(2)	*x,y,z*
N5–H5•••N4	3.047(5)	2.187(3)	177.67(3)	*-x,+y,-z+1/2*
C5–H5A•••O2	3.633(7)	2.712(4)	161.13(4)	*x-1/2,+y-1/2,+z*
		AMT-NO3		
N1–H1•••O1	2.748(3)	1.890(2)	175.78(2)	*x,y,z*
N1–H1•••O2	3.490(3)	2.826(3)	135.20(2)	*x,y,z*
N2–H2•••O2	2.889(3)	2.036(3)	171.20(2)	*x,y,z*
C9–H9B•••O1	3.452(4)	2.579(2)	151.24(2)	*-x,-y+1,-z+2*
C9–H9B•••O3	3.466(4)	2.592(3)	151.48(2)	*-x,-y+1,-z+2*
C8–H8C•••O3	3.679(7)	2.781(3)	156.03(3)	*-x,-y+2,-z+1*
		AMT-TFA		
N1–H1•••O1	2.643(3)	1.784(3)	176.16(2)	*x,y,z*
N2–H2•••O2	2.974(3)	2.117(2)	173.59(2)	*x,y,z*
N5–H5•••O2	3.146(4)	2.361(3)	151.98(2)	*x,-y+1/2,+z-1/2*
C9–H9B•••F3	3.634(7)	2.859(4)	138.44(3)	*x,-y+1/2,+z-1/2*
C5–H5A•••F2	3.347(7)	2.594(4)	135.52(3)	*x,-y+1/2,+z-1/2*
C8–H8C•••F2	3.655(6)	2.834(3)	143.96(3)	*-x+1,+y-1/2,-z+1/2+1*
C7–H7A•••F2	3.561(6)	2.713(4)	147.56(3)	*-x+1,+y-1/2,-z+1/2+1*
C9–H9C•••O1	3.786(6)	2.828(3)	175.58(3)	*-x+2,-y+1,-z+1*
C5–H5B•••F1	3.666(6)	2.904(3)	137.07(3)	*x-1,-y+1/2,+z-1/2*

Table S3. pKa values for atrazine, ametryn, and multicomponent formers

Compound	**pK_a**
Ametryn	4.0[2]
Atrazine	1.7[2,3]
Fumaric acid (H_2Fum)	3.03 and 4.44[4]
Nitric acid (HNO_3)	-1.5[5]
Trifluoracetic acid (3FAH)	0.52[6]
Malic acid	3.4, 5.2 and 14.5[7]
Oxalic acid	1.27 and 4.27 [8]

Table S4. Principal FT-IR bands (cm^{-1}) for ATZ and AMT multicomponent crystals

Assignment (cm^{-1})	**ATZ**	**ATZ-H_2Fum**	**AMT**	**AMT-NO_3**	**AMT-TFA**
ν(N−H)	3257, 3103	3269, 3210	3251, 3093	3261, 3095	3269, 3083
ν(C−H)	2972, 2931	2972, 2935	2968, 2933	2972, 2929	2981, 2939
ν(C=O)	-	1701	-	-	-
ν($C_3N_{3\ ring}$)	1618, 1546	1620, 1558	1606, 1523	1658, 1612	1679, 1608
ν(COO^-)	-	-	-	-	1559, 1443
ν(C=N)	1338	1344	1334	1332	1346
ν(NO_3^-)	-	-	-	1382, 1160	-
ν(C−S)	-	-	1001	999	995
δ(C−H)	808	800	806	806	790
ν(C−Cl)	690	692	-	-	-

Table S5. Equilibrium solubility values (mg mL^{-1}) of ATZ cocrystal and AMT salts. The ATZ and AMT were added for comparison purpose.

Compound	Solubility (mg mL^{-1})
ATZ	0.682
ATZ-H_2Fum	3.88
AMT	0.215
AMT-NO_3	4.50
AMT-TFA	2.96

Figure S1. View of the asymmetric unit (ASU) of (a) ATZ-Fum (C2/c, Z'=1), (b) ATZ-H_2Fum.H_2O (C2/c, Z'=1), (c) AMT-NO3 ($P\bar{1}$, Z'=1), (d) AMT-3FA (P21/c, Z'=1).

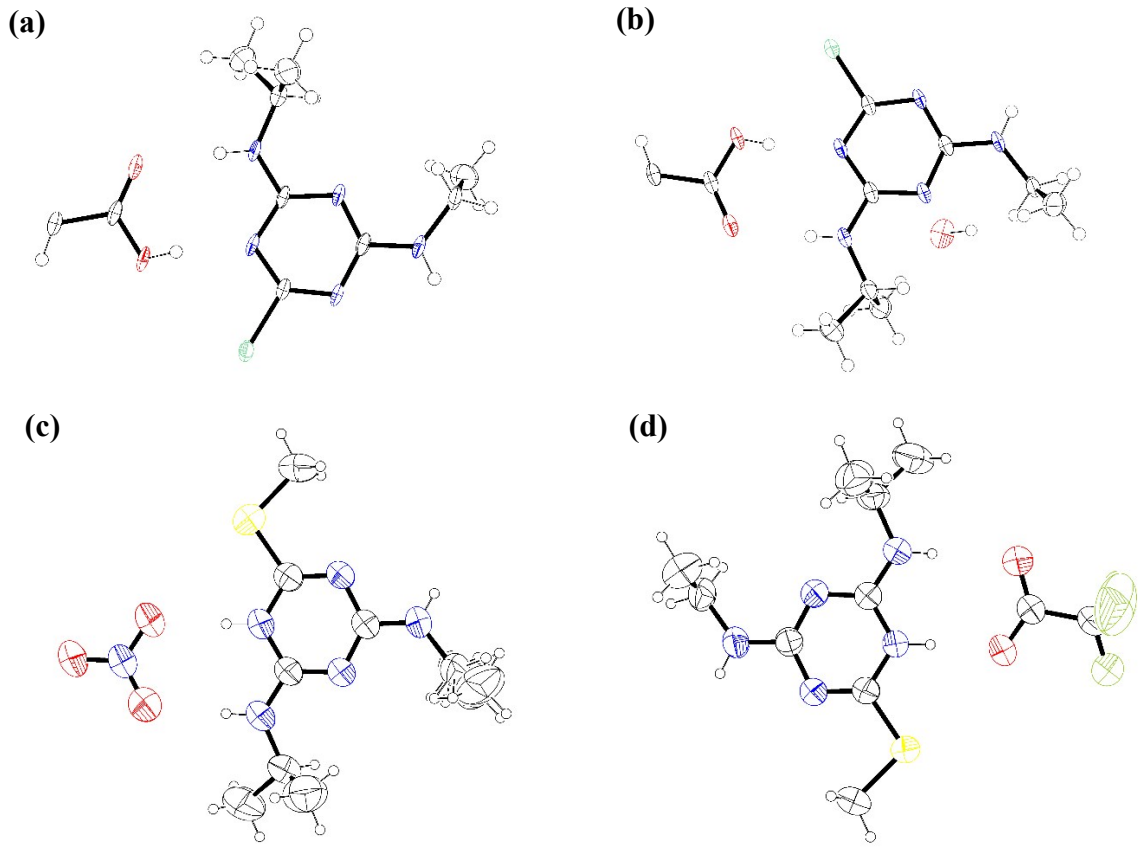

Figure S2. The isostructural packing of (a) ATZ-H2FumH2O and the (b) dehydrates ATZ-H2Fum. The coexistence of isostructural hydrate and dehydrated phases have identified as outcome of the crystallization. Notably, the ATZ-Fum H_2O structure showed poor thermal stability, releasing the water molecules below 330 K converting into the isostructural dehydrate. This type of hydrate occurs owing to the structure formed be able to generate channels that allow the flow of water molecules with low retention.

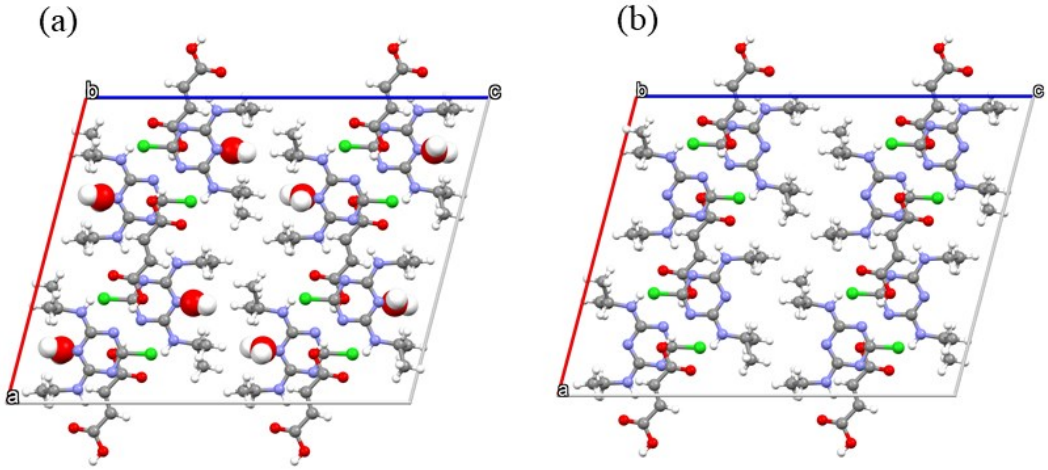

Figure S3. Fourier difference map for the neutral ATZ molecule in the (a) ATZ-H_2Fum.H_2O and (b) ATZ-H_2Fum cocrystals. And for the AMT^+ cation in (c) AMT-NO3 and (d) AMT-TFA salts. The cocrystal formation is confirmed by the non-protonation of COOH groups of the fumaric acid. In the ametryn salts, it has seen the protonation of AMT molecule on the N5-atom for both cases.

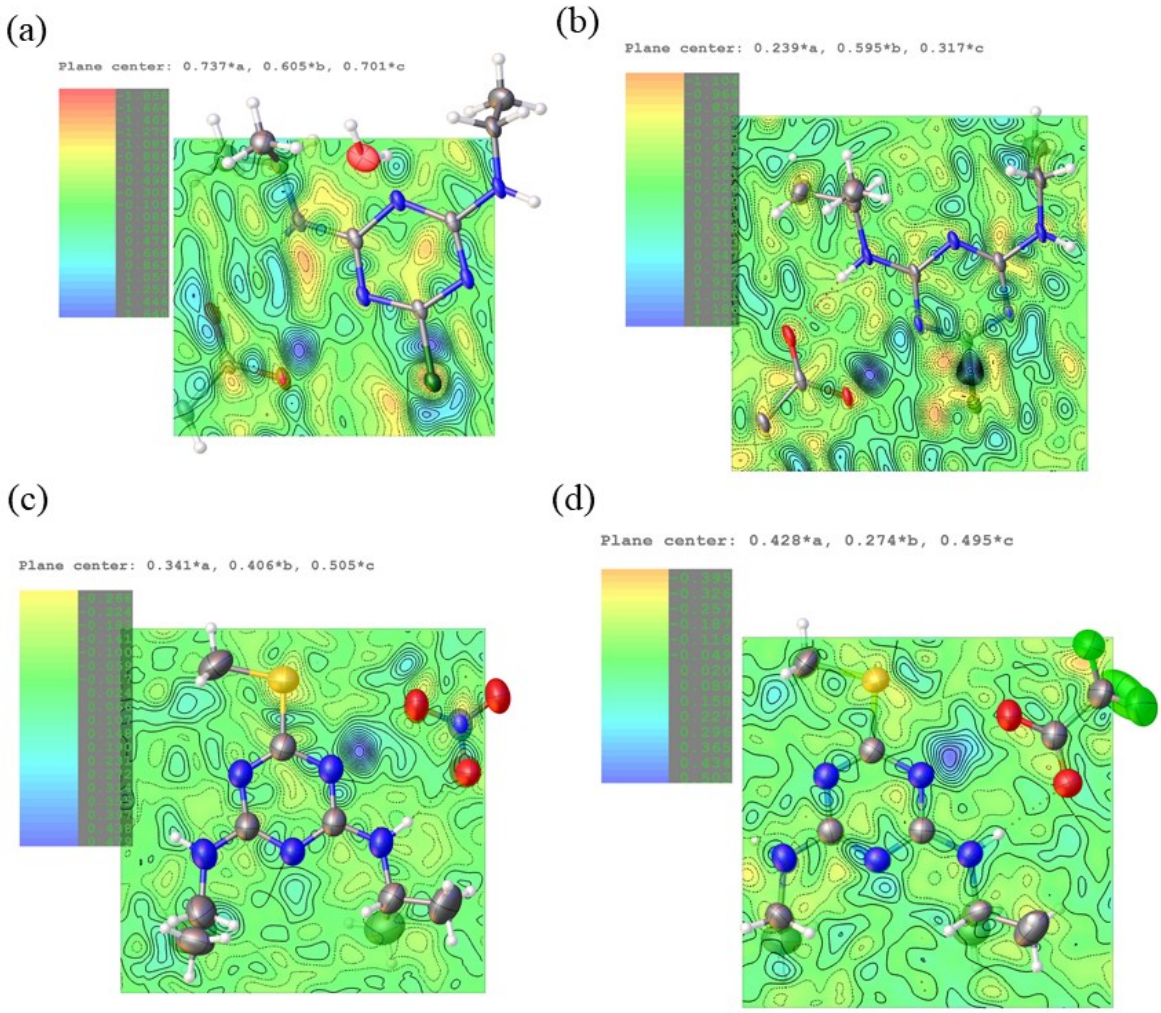

Figure S4. The ATZ-H_2Fum·H_2O parking. The association between the water and ATZ molecules are highlighted in the blue square.

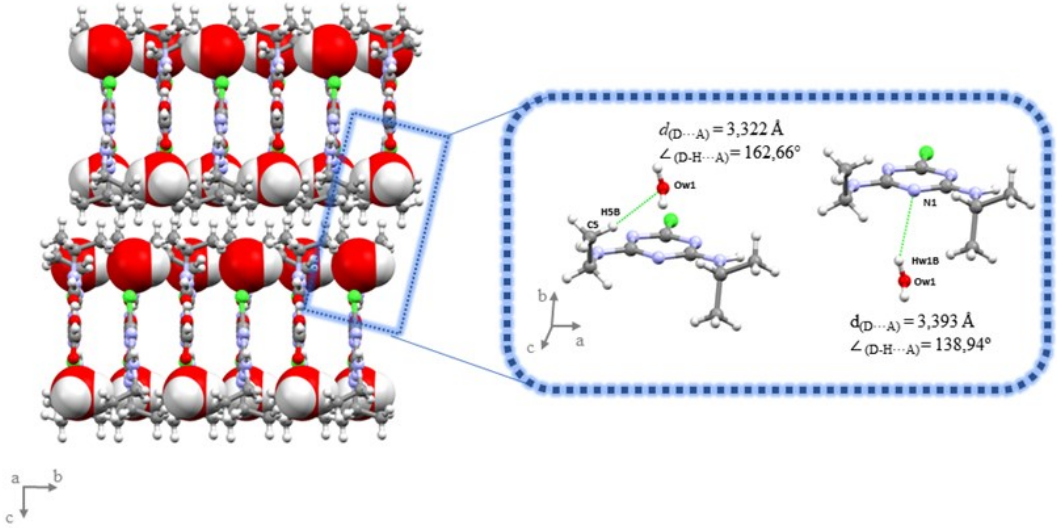

Figure S5. (a) The amino-triazine···H_2Fum and amino-triazine···amino-triazine synthons along to axis 100. (b) projection of chains arranged in opposite positions along the axis 010 forming crystalline packaging.